Relationship Between Cortical Thickness and Functional Activation in the Early Blind

Irina Anurova[1,2], Laurent A. Renier[1,3], Anne G. De Volder[3], Synnöve Carlson[2,4] and Josef P. Rauschecker[1]

[1]Laboratory of Integrative Neuroscience and Cognition, Department of Neuroscience, Georgetown University Medical Center, Washington, DC 20057, USA, [2]Neuroscience Unit, Institute of Biomedicine/Physiology, University of Helsinki, Helsinki 00014, Finland, [3]Institute of Neuroscience, Université Catholique de Louvain, Brussels B-1200, Belgium and [4]Brain Research Unit, O. V. Lounasmaa Laboratory, Aalto University School of Science, Aalto 00076, Finland

Address correspondence to Josef P. Rauschecker, Department of Neuroscience, Georgetown University Medical Center, New Research Building WP 19, 3970 Reservoir Road, Washington, DC 20057, USA. Email: rauschej@georgetown.edu

Early blindness results in both structural and functional changes of the brain. However, these changes have rarely been studied in relation to each other. We measured alterations in cortical thickness (CT) caused by early visual deprivation and their relationship with cortical activity. Structural and functional magnetic resonance imaging was performed in 12 early blind (EB) humans and 12 sighted controls (SC). Experimental conditions included one-back tasks for auditory localization and pitch identification, and a simple sound-detection task. Structural and functional data were analyzed in a whole-brain approach and within anatomically defined regions of interest in sensory areas of the spared (auditory) and deprived (visual) modalities. Functional activation during sound-localization or pitch-identification tasks correlated negatively with CT in occipital areas of EB (calcarine sulcus, lingual gyrus, superior and middle occipital gyri, and cuneus) and in nonprimary auditory areas of SC. These results suggest a link between CT and activation and demonstrate that the relationship between cortical structure and function may depend on early sensory experience, probably via selective pruning of exuberant connections. Activity-dependent effects of early sensory deprivation and long-term practice are superimposed on normal maturation and aging. Together these processes shape the relationship between brain structure and function over the lifespan.

Keywords: blindness, cortical thickness, cross-modal plasticity, magnetic resonance imaging (MRI), pruning

Introduction

It is well established that visual deprivation causes structural and functional reorganization in both the deprived and the intact sensory cortices (Rauschecker 1995; Bavelier and Neville 2002; Merabet and Pascual-Leone 2010). Although functional and structural changes after sensory deprivation have been studied extensively (Gilbert and Wiesel 1992), relatively little is known about how these changes relate to each other.

Sensory areas of the deprived modality have been shown consistently to adopt an important role in the processing of information from intact modalities during perceptual (Weeks et al. 2000; Pietrini et al. 2004; Kujala et al. 2005; Voss et al. 2008) and cognitive tasks (Sadato et al. 1996, 1998; Cohen et al. 1997; Büchel et al. 1998; Hamilton and Pascual-Leone 1998; Röder et al. 2002; Burton et al. 2003; Bedny et al. 2011; Striem-Amit et al. 2012). Recruitment of occipital cortex during nonvisual processing in the blind has been shown to be related to successful behavioral performance, since the degree of occipital involvement correlates positively with Braille reading abilities (Cohen et al. 1997), sound localization accuracy (Gougoux et al. 2005), and verbal memory performance (Amedi et al. 2003).

Increased cortical thickness (CT) within the occipital lobes in congenitally blind (CB) and early blind (EB) but not in late blind (LB) individuals compared with sighted controls (SC) is among the most consistently reported morphological changes caused by visual deprivation (Bridge et al. 2009; Jiang et al. 2009; Park et al. 2009; Voss and Zatorre 2011). Furthermore, it has recently been shown that occipital CT correlates positively with enhanced performance of the EB in a transposed melody discrimination task (Voss and Zatorre 2011). Thus, assuming that enhanced performance correlates positively with cortical activation (e.g., Cohen et al. 1997; Gougoux et al. 2005; Amedi et al. 2003; Karni et al. 1995), it would be logical to expect that CT within the occipital lobes of the EB also correlates positively with the magnitude of activation, that is, thicker cortex should be activated more strongly and vice versa.

On the other hand, it has been argued that greater thickness of occipital cortex in the EB may be caused by reduced pruning of exuberant connections (axon collaterals, dendritic arbors) and reduced elimination of ineffective synapses, which normally takes place during early development, with amount of pruning dependent on visual experience (Jiang et al. 2009). Although the initial connectivity of the visual pathway is nearly complete by the end of the gestation period, visual experience is still a key factor for synaptic refinement and increasing neurocomputational abilities (Innocenti and Frost 1979; Innocenti and Price 2005; Sanes et al. 2006). Deprived of visual stimulation, the occipital cortex of EB and CB individuals remains thicker compared with that of sighted. Owing to involvement of blind occipital areas in processing nonvisual information, however, these areas still undergo selective refinement by elimination of exuberant connections and stabilization of effective synapses ("Hebbian" plasticity; Rauschecker 1991). Therefore, within the group of EB, areas with a thinner cortex should be associated with more effective function, so negative correlations between CT and magnitude of activation might be expected. Consistent with this prediction, most studies in which relationships between cortical structure and function have been tested suggest a negative correlation between CT and activation in typically developing children and adults, that is, thinner cortex is activated more strongly (Rasser et al. 2005; Lu et al. 2009; Nunez et al. 2011). To our knowledge, only one study has shown a positive correlation between CT and functional activation in a limbic structure, the anterior cingulate cortex (Hegarty et al. 2012).

The present study was designed to resolve this ambiguity by measuring regional changes in CT caused by early blindness in relation to activation during functional magnetic resonance imaging (fMRI). Correlations between CT and magnitude of activation associated with auditory processing of sound

identity and spatial location in both EB and SC were analyzed at the whole-brain level and within several anatomically defined regions of interest, including primary and nonprimary areas of visual and auditory cortex. This approach aimed to reveal whether and how the relationship between structure and function depends on early visual experience. Overall, we expected to find evidence for neuroplastic changes in cortical areas of EB subjects for both deprived (visual) and intact (auditory) modalities. We hypothesized that some occipital areas in EB would be activated particularly during demanding auditory tasks, similar to how nonprimary auditory areas are activated in SC. Consequently, we expected that relationships between anatomical structure and function typical for nonprimary auditory cortex in SC would also be observed in the reorganized "visual" cortex of the EB during auditory information processing. More specifically, we expected to find correlations between structure and function within equivalent cortical areas when attention is directed to spectral or spatial characteristics of the sounds. Two recent studies (Renier et al. 2010; Collignon et al. 2011), for instance, emphasized a specific role for the middle occipital gyrus (MOG), known to be involved in the processing of visual spatial information in the sighted, and of auditory spatial information in EB individuals. Based on these findings, we hypothesized that, in the EB, significant correlations between CT and functional activation during an auditory spatial task would be observed within the MOG.

Materials and Methods

Subjects
Anatomical and functional neuroimaging data were obtained from 12 EB (5 males, 10 right-handed, mean age ± standard deviation [S.D.]: 49 ± 9.2 years) and 12 age-, gender-, and handedness-matched sighted volunteers (mean age ± S.D.: 45 ± 10.9 years), which served as controls. All participants were healthy, with no history of neurological or psychiatric disorders. Nine of the blind participants were totally blind from birth and 3 became blind by the second year of life. Clinical characteristics of blind subjects are presented in Table 1. The study protocol was approved by Georgetown University's Institutional Review Board; written informed consent was obtained from all participants prior to the experiment.

Data Acquisition
All neuroimaging data were acquired at Georgetown University's Center for Functional and Molecular Imaging on a 3-Tesla Siemens Tim Trio scanner equipped with a 12-channel head coil. The fMRI data were acquired using an echo-planar imaging sequence (flip angle = 90°, TR = 3 s, TE = 60 ms). The FOV was 192×192 mm^2 with a 64×64

Table 1
Clinical characteristics of EB subjects

Subject	Sex	Age (years)	Handedness	Cause of blindness	Onset of blindness
EB01	M	56	Right	ROP	Congenital
EB02	M	45	Right	Retinopathy	<2 years
EB03	F	56	Right	Unknown	Congenital
EB04	M	38	Right	Retinal detachment	<2 years
EB05	F	58	Right	ROP	Congenital
EB06	M	53	Right	ROP	Congenital
EB07	M	55	Right	Retinal detachment	Congenital
EB08	F	34	Right	Optic nerve hypoplasia	<2 years
EB09	F	34	Right	ROP	Congenital
EB10	F	55	Left	ROP	Congenital
EB11	F	55	Right	ROP	Congenital
EB12	F	56	Left	ROP	Congenital

ROP, retinopathy of prematurity; M, male; F, female.

matrix size; slice thickness was 2.8 mm with a 0.2-mm gap, resulting in an effective voxel resolution of $3 \times 3 \times 3$ mm^3. For each run, 184 volumes of 50 slices were acquired in a continuous sampling paradigm. At the end, a high-resolution 3D T_1-weighted MPRAGE image (resolution $1 \times 1 \times 1$ mm^3) was acquired for each subject (TR = 1900 ms, TE = 2.52 ms, TI = 900 ms, flip angle = 9°). The volume consisted of 176 sagittal slices (FOV = 256×256 mm^2, 256×256 matrix, slice thickness = 1 mm).

Stimuli and Experimental Design
The stimuli were 4 C-major piano chords over a range of 4 octaves originating from 4 different locations in virtual auditory space. The stimuli were presented via electrostatic MRI-compatible headphones (STAX, frequency transfer function 20 Hz to 20 kHz). Four sound source locations, ±90° (corresponding to the extreme left and right) and ±30°, were simulated by convolving the stimuli with standard head-related transfer functions provided by Amphiotik Synthesis. The stimulus duration was 1000 ms (including 10 ms rise/fall times); the interstimulus interval was 1 s.

Subjects performed auditory identification (ID), localization (Loc), and simple sound-detection (SD) tasks. The experimental setup was the same as that used in Renier et al. (2010). For both auditory ID and Loc conditions, a one-back paradigm was employed. In this paradigm, subjects had to compare each new stimulus in the sequence with the previous one and categorize it as either the same or different regarding a certain stimulus attribute. During the ID task, subjects compared the chords in terms of pitch height, while, in the Loc task, they compared the chords' spatial locations. In matching trials, subjects pressed the left button of the MRI-compatible response pad with the left middle finger; in nonmatching trials, they pressed the right button with the left index finger. During the SD task, subjects pressed the left button every time they heard a stimulus. The SD task was used to control for perceptual and motor components of the experimental tasks (ID and Loc). In the ID task, spatial locations of the sounds were fixed within one condition, but varied among conditions. Conversely, in the Loc task, the same chord was presented from different locations, whereas the chord's height varied from one condition to another. In the SD task, both the chords' pitch and their spatial locations were fixed. The onset of each condition was announced through the headphones. Presentation of the stimuli and collection of behavioral data were controlled by Superlab software 4.0 (Cedrus Corp.). Sighted subjects were blindfolded during the scanning session. Before scanning, all participants were familiarized with the tasks during a brief practice session. Acquisition of functional data was performed using a block-design paradigm. Duration of 1 block was 18 s and corresponded to 9 presentations of stimuli. Blocks were separated by 12-s resting periods. Each of the 3 experimental conditions (ID, Loc, and SD) was repeated 6 times during a 9-min run. Thus, 1 run consisted of 18 blocks. Three runs were presented during the experiment. The order of the experimental conditions was counterbalanced across subjects.

Statistical Evaluation of Behavioral Data
Analysis of behavioral data (percent correct responses) was performed with a two-way mixed-design ANOVA with Group (EB vs. SC) as a between-subjects factor and Task (ID vs. Loc) as a within-subject factor. Detection scores were compared between the 2 groups using the two-tailed unpaired t-test.

Structural and Functional MRI Data Processing
Analysis of both structural (CT) and functional data was performed in surface space using Brain Voyager 2.1 (BVQX, Brain Innovation, Maastricht, the Netherlands).

Cortical Reconstruction and Intersubject Alignment
An intersubject cortical alignment procedure was employed in order to reduce the effect of anatomical variability and to improve the spatial correspondence of cortical areas between individual brains. Prior to surface reconstruction, the original T_1-weighted MRIs were corrected for spatial intensity inhomogeneities and then converted into volumes

with 1-mm isotropic voxels. After that, the volumes were further spatially transformed into standard Talairach space. Sinc interpolation was used at all steps of spatial transformation. For the normalized MRIs, an automatic segmentation of white-matter (WM) and gray-matter (GM) boundaries was applied. Topological errors such as "bridges" and remaining fragments of dura mater or cerebellum were corrected manually. The reconstructed cortical hemispheres were morphed into spherical representations of the folded cortex. Curvature information of individual brains was used for cortex-based intersubject alignment, which was carried out using the moving-target group averaging (Goebel et al. 2006) and resulted in creating averaged curvature maps. After the alignment procedure, averaged folded meshes were constructed for both hemispheres. Each mesh resulted from averaging 24 individual datasets (12 EB and 12 SC). These meshes were used for projecting both anatomical (CT) and functional (fMRI) datasets.

CT Analysis
CT analysis was carried out following a series of advanced segmentation steps. First, the Talairach-transformed individual MRIs were resampled to 0.5-mm isovoxel resolution space using sinc interpolation. Brains were segmented from the head tissue using an automatic brain-peeling tool. Peeling parameters were individually adjusted for each subject's MRI. Subcortical structures and cerebellum were removed using a default brain mask. Then, tissue contrast and homogeneity enhancement were followed by segmentation of WM/GM and GM/cerebrospinal fluid boundaries. After segmentation of the cortical layer was completed, CT was measured for each subject's hemisphere using the Laplace method (Jones et al. 2000; Geuze et al. 2008). Averaged CT maps were generated separately for each group of subjects. Whole-brain group differences in CT were evaluated using a two-tailed unpaired t-test in cortical surface space following cortical reconstruction and intersubject alignment. The results were corrected for multiple comparisons by cluster-size correction analysis, incorporated in Brain Voyager QX, using a Monte Carlo simulation procedure with 1000 iterations in order to define the cluster-size threshold corresponding to a familywise error rate of 0.05.

In a subsequent region-of-interest (ROI) analysis, we compared averaged thickness values from anatomically defined ROIs across subjects. Each ROI was determined on the basis of averaged meshes using anatomical landmarks. In the occipital lobes, ROIs were located within primary and nonprimary visual areas including bilateral calcarine sulcus (CS), lingual gyrus (LG), cuneus (Cu), and lateral occipital (LO) cortex. The LO region included the lateral surface of the occipital lobes (middle and inferior occipital gyri, MOG and IOG, respectively) bounded superiorly by the LO sulcus and anteriorly by the anterior occipital sulcus and temporo-occipital incisura (Fig. 2*A*). The ROIs within the temporal lobes included bilateral Heschl's gyrus (HG), and bilateral anterior and posterior parts of the lateral convexity of the superior temporal gyrus extending anteriorly and posteriorly to HG, respectively (aSTG, pSTG) (Fig. 2*B*). Statistical evaluations of CT were done separately for each pair of corresponding ROIs in the left and right hemispheres using a two-way analysis of variance (ANOVA) with Group (EB vs. SC) as a between-subjects factor and Hemisphere (left and right) as a within-subject factor. Mean CT values over each ROI were used as dependent variables. If significant main effects were observed ($P < 0.05$), post hoc analyses were performed using the Newman–Keuls test.

Analysis of Functional Data
The preprocessing of the functional data included slice-timing correction, correction for small interscan head movements, temporal high-pass filtering (removing frequencies lower than 3 cycles/run), and spatial smoothing using a 6-mm Gaussian filter. Data were transformed into Talairach space (Talairach and Tournoux 1988). For anatomical reference, the computed statistical maps were overlaid on the 3D T_1-weighted scans. A general linear model (GLM) was used to analyze the blood oxygen level–dependent (BOLD) responses of each subject as a function of experimental condition. Regressors of interest consisted of boxcar functions convolved with the standard hemodynamic response function. A random-effects analysis of variance (RFX ANOVA) was employed in order to remove intersubject variability. The RFX ANOVA was applied in cortical surface space following the cortical

reconstruction and intersubject alignment. The whole-brain analysis was done in 2 steps. First, BOLD responses associated with each experimental condition (ID, Loc, and SD) were compared between the 2 groups (EB vs. SC). Second, BOLD responses evoked by one-back tasks compared with the control task ((ID + Loc) vs. SD) were computed separately for each group. For all contrasts, the P values were corrected for false discovery rate (FDR) using a threshold of $q < 0.05$. The results of the direct contrast between the ID and Loc tasks were described in detail in an earlier paper from our group that focused on the differences between spatial and nonspatial processing in EB (Renier et al. 2010).

In the ROI analyses, statistical evaluations of the magnitude of the BOLD response were performed separately for each pair of corresponding ROIs in the left and right hemisphere using a three-way ANOVA with Group (EB vs. SC) as a between-subjects factor and Task (ID, Loc, and SD) and Hemisphere (left and right) as within-subject factors. The mean percentages of signal change over the ROI were used as dependent variables. The Greenhouse–Geisser correction was used for factors with more than 2 levels. If significant main effects were observed ($P < 0.05$), post hoc analyses were performed using the Newman–Keuls test.

Analysis of Correlations Between CT and Activation and Between CT and Age
First, in order to identify a general tendency in the relationships between CT and regional BOLD responses, we created a mixed-effects GLM, in which percent signal change within the ROIs during the ID, Loc, and SD tasks were used as dependent variables, CT and age as continuous predictors, and Group (EB vs. SC), ROI and Hemisphere (left vs. right) as categorical predictors. BOLD responses elicited during the ID, Loc, and SD tasks were tested separately. Wald-type statistics were applied to test the effects of CT and its interactions with other factors and their combinations. For tasks in which CT × Group × ROI × Hemisphere interactions produced significant main effects, the relationships between CT and activation were further tested using a GLM separately for each ROI (left and right) and each group of subjects. All statistical tests with subjects treated as random-effects were also controlled for Age. Finally, the ROIs where CT produced a significant effect on activation were submitted for the next step of analysis, in which relationships between the CT and BOLD response were tested using Pearson's correlations.

In addition to the GLM analysis in which mean values for the CT and percent signal change within each ROI were used, the relationships between CT and regional BOLD responses were examined at the whole-brain level in surface space using BVQX. Pearson's correlation coefficients (r) were calculated at each cortical surface point (vertex by vertex). The r-maps were corrected for multiple comparisons by cluster size using a Monte Carlo simulation.

Correlations between CT and age/duration of blindness were studied separately for each ROI and each group of subjects by using Pearson's correlation analyses.

Results

Differences between EB and SC participants were assessed in terms of 1) behavioral performance, 2) anatomy (CT), and 3) functional activation (BOLD response). Finally, a correlation between CT and activation data was performed.

Behavioral Data

Accuracy of one-back ID and Loc task performance did not differ between groups ($F_{1,22} = 0.8$, $P = 0.37$) or tasks ($F_{1,22} = 1.1$, $P = 0.31$). Both EB and SC participants managed pitch-identification and sound-localization tasks at high accuracy levels, though not at ceiling (EB, 87 ± 2% (mean ± standard error of mean) for the ID task and 85 ± 3% for the Loc task; SC, 89 ± 2% and 89 ± 3%, respectively). Detection scores in a sound-detection task (SD), which was used as a control task,

were nearly perfect and did not differ between groups (99 ± 1% in EB and 97 ± 2% in SC; $t_{(22)} = 0.9$, $P = 0.38$).

CT Analysis

CT Analysis of Whole-Brain Data

Comparison of CT data from EB and SC participants was first performed in a whole-brain analysis, followed by analysis of anatomically defined ROIs in occipital and superior temporal regions to specifically study effects in visual and auditory areas.

A *t*-test revealed significant group differences in CT between EB and SC ($P < 0.05$, corrected for multiple comparisons by cluster size) throughout a wide range of cortical areas (Fig. 1, Table 2). The most prominent differences were observed in occipital and frontal regions. Smaller clusters of group differences in CT were also detected within the right superior parietal lobe and in anterior cingulate gyrus. In all these areas, cortex was thicker in the EB group.

CT Analysis of ROI Data

A more detailed analysis of CT was performed for different anatomical regions in occipital and superior temporal regions, as defined in Materials and Methods (Fig. 2A,B).

In occipital ROIs, cortex was consistently thicker in EB than in SC subjects, confirming the results of whole-brain analysis. Using two-way ANOVA, a significant main effect of Group was observed within the CS ($F_{1,22} = 5.5$, $P < 0.05$), LG ($F_{1,22} = 4.3$, $P < 0.05$), Cu ($F_{1,22} = 9.6$, $P < 0.01$), and LO regions ($F_{1,22} = 7.0$, $P < 0.05$).

In superior temporal ROIs, corresponding to auditory regions, the effects of early blindness on CT were less uniform. A significant main effect of Group was found in anterior STG (aSTG) ($F_{1,22} = 5.1$, $P < 0.05$), where cortex was thinner in EB than in SC. In HG, corresponding to primary auditory areas, CT showed a Group–Hemisphere interaction ($F_{1,22} = 4.3$, $P < 0.05$) indicating that left HG was thicker in the group of EB than SC ($P < 0.05$). No significant effects of Group ($F_{1,22} = 0.14$,

$P = 0.71$) and no Group–Hemisphere interactions ($F_{1,22} = 0.01$, $P = 0.92$) were detected for posterior STG (pSTG) (Fig. 2C).

Functional MRI Data Analysis

Whole-Brain fMRI Data

Group differences (EB vs. SC) in cortical functional activation corresponding to each experimental task (ID, Loc, SD) are presented in Figure 3 and Table 3.

In the auditory ID task, significant group differences were observed within medial and LO cortex, including the CS, LG, Cu, and inferior/middle occipital gyri (IOG/MOG). In all regions of occipital cortex, activation by the auditory ID task was stronger in the group of EB than in SC. Decreased activation in EB compared with SC was observed in the medial part of left HG, and within right superior temporal sulcus (STS).

In the auditory Loc task, enhanced activation in the EB group was observed within the same general regions of occipital cortex, within the superior parietal lobes bilaterally, and within the left middle frontal gyrus/sulcus.

In the SD task, group differences between EB and SC were confined to a small cluster within the right central sulcus (Table 3).

Contrasting cortical activation during the more demanding ID and Loc tasks with activation corresponding to the simple SD task revealed both similarities and differences between the EB and SC groups (Fig. 4, Table 4). Areas activated more strongly during the one-back tasks (compared with SD) included the fronto-parietal network in both groups, the medial and LO areas in the group of EB subjects, and nonprimary auditory cortex within pSTG for the group of SC. Task-induced deactivation was observed for both groups in areas of the "default-mode network" (Buckner et al. 2008), including medial frontal and parietal areas, anterior and posterior cingulate cortex, inferior parietal lobule, and lateral anterior temporal areas extending to the temporal pole. In addition, auditory one-back tasks induced deactivation within the right
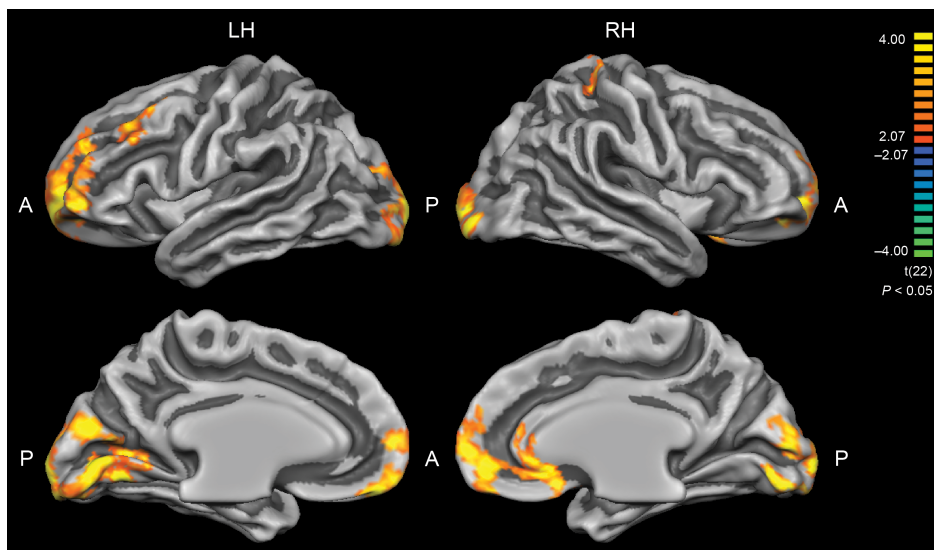

Figure 1. Group differences in cortical thickness (EB > SC). Results are shown at $P < 0.05$, corrected by cluster size. Color scale codes *t* values. LH, left hemisphere; RH, right hemisphere; A, anterior; P, posterior. Occipital and frontal areas in EB were significantly thicker than in SC subjects (see Table 2).
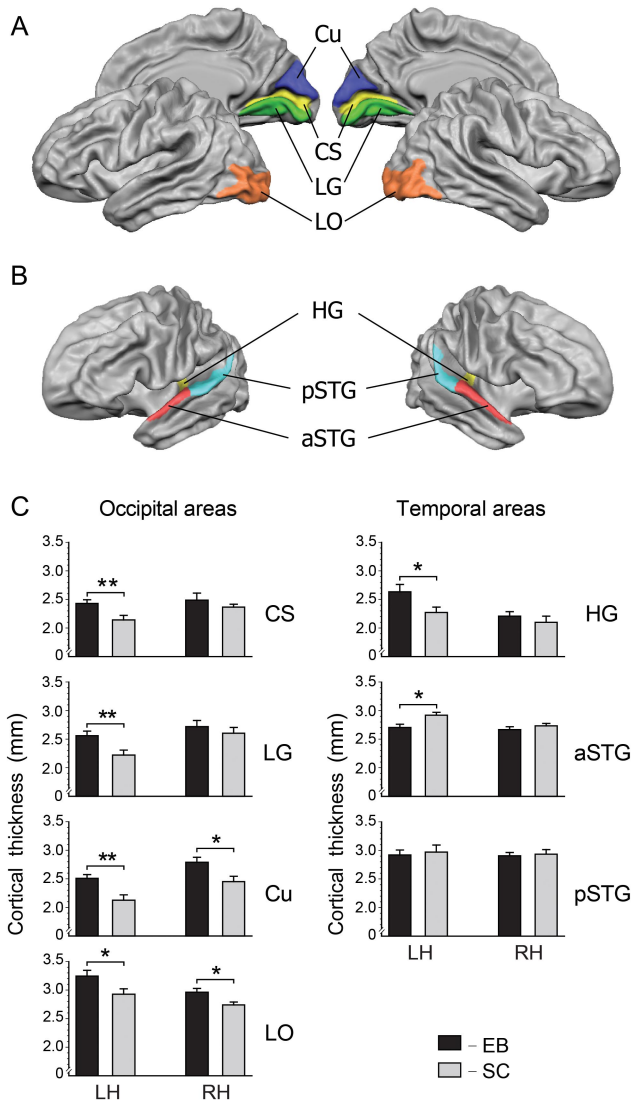
Figure 2. Anatomically defined ROIs in occipital (*A*) and superior temporal (*B*) cortices. (*C*) Cortical thickness within anatomically defined ROIs in EB (black bars) and SC (gray bars) subjects. Cu, cuneus; CS, calcarine sulcus; LG, lingual gyrus; LO, lateral occipital cortex; HG, Heschl's gyrus; aSTG, pSTG, anterior/posterior parts of the superior temporal gyrus; *P < 0.05, **P < 0.01. In occipital areas, cortex is consistently thicker in EB than in SC. In superior temporal areas, primary auditory cortex in the left HG was thicker, while nonprimary auditory cortex in the left aSTG was thinner in EB compared with SC.

Table 2

Brain regions showing significant group differences in CT in a whole-brain analysis

Brain region	BA	x	y	z	t value	P value
L LG	17	−4	−77	0	8.09	<0.000001
L Cu	18	−5	−82	19	4.89	<0.0001
L MOG	17/18	−15	−98	−3	7.32	<0.000001
L IOG	18	−19	−94	−15	4.75	<0.0001
L CS	17	−20	−62	5	3.95	<0.001
L SFG	10	−22	53	10	5.94	<0.00001
L MFG	10/46	−36	52	2	4.83	<0.0001
L MFG	9	−33	25	38	3.59	<0.005
R LG	18	3	−76	−3	5.13	<0.00005
R Cu	17	6	−84	7	5.03	<0.00005
R IOG	18	28	−90	−3	6.64	<0.000001
R SFG/SFS	10	18	55	4	5.12	<0.00005
R ACG	32	6	45	−1	5.50	<0.00005
R PoCeG/PoCeS	5	24	−37	54	3.92	<0.001

BA, Brodmann area; x, y, z, peak Talairach coordinates; ACG, anterior cingulate gyrus; CS, calcarine sulcus; Cu, cuneus; IOG, inferior occipital gyrus; LG, lingual gyrus; MFG, middle frontal gyrus; MOG, middle occipital gyrus; PoCeG, postcentral gyrus; PoCeS, postcentral sulcus; SFG, superior frontal gyrus; SFS, superior frontal sulcus.
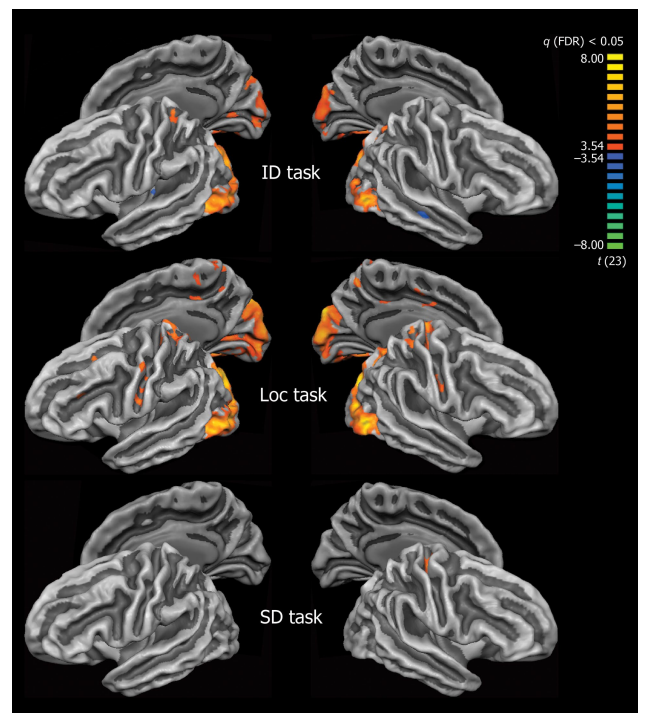

Figure 3. Group differences in cortical functional activation (EB > SC) during Identification versus Rest (ID), Localization versus Rest (Loc), and Sound Detection versus Rest (SD) tasks. Group differences are shown at *P* < 0.05, FDR-corrected. Color scale codes *t* values. ID and Loc auditory one-back tasks, but not SD, produce stronger activation in the occipital cortex in EB compared with SC.

LO cortex in the group of SC, which was activated in the group of EB.

Region-of-Interest fMRI Data

Results of the ROI analysis of the fMRI data are presented in detail as Supplementary Material. In brief, in the group of EB, occipital cortex was activated consistently more strongly than in SC during auditory ID and Loc one-back tasks, confirming the results of whole-brain analysis (Supplementary Fig. 1).

In auditory areas, a group difference in the magnitude of activation was observed in the ID task only: for the group of SC, HG was activated significantly more strongly than for EB. Furthermore, as might be expected, HG activation was not significantly modulated by the type of task in either of the groups. In contrast, activity within nonprimary auditory areas was task dependent for SC: aSTG was activated more strongly during the ID than Loc task, and pSTG was activated more strongly during both ID and Loc tasks than during simple SD. In EB, activity within anterior and pSTG was less specific.

Correlation Between Cortical Thickness and fMRI Activation

For studying the relationship between CT and functional activation, we employed a mixed-effects GLM and looked specifically for [CT × Group × ROI] and [CT × Group × ROI × Hemisphere]

Table 3
Brain regions showing significant group differences in activation by auditory stimuli across experimental tasks in a whole-brain analysis

Experimental task	Brain region	BA	x	y	z	t value	P value
ID Task (EB > SC)	L Cu/SOG	18	−13	−90	18	6.44	<0.000001
	L Cu	17/18	−6	−82	12	4.66	<0.0005
	L IOG/MOG	18/19	−39	−78	1	6.15	<0.000005
	L FG	19	−33	−63	−13	5.08	<0.00005
	L CS	17	−10	−88	−3	4.23	<0.0005
	L LG	18	−14	−75	−9	4.11	<0.0005
	L PoCeS	5	−18	−43	58	4.05	<0.0005
	R Cu	18	7	−82	24	5.09	<0.0005
	R SOG	18/19	18	−82	25	6.41	<0.000005
	R MOG	18	29	−83	7	5.33	<0.00005
	R IOG	18/19	43	−71	−1	7.72	<0.000001
	R CS	17	9	−82	1	4.52	<0.0005
	R LG	17	17	−62	4	4.91	<0.0001
	R FG	19	29	−66	−13	5.68	<0.00001
	R SPL	7	22	−63	45	4.51	<0.0005
ID Task (EB < SC)	L HG	41	−40	−22	8	−4.28	<0.0005
	R MTG	21	52	−21	−7	−4.72	<0.0001
Loc Task (EB > SC)	L Cu	17	−5	−84	10	6.20	<0.000005
	L SOG	19	−19	−82	27	7.74	<0.000001
	L MOG	19	−26	−85	5	6.56	<0.000005
	L CS	17	−7	−87	2	5.27	<0.00005
	L LG	18	−12	−80	−13	4.83	<0.0001
	L FG	19	−25	−63	−13	5.50	<0.00005
	L SFS	6	−24	13	44	4.06	<0.0005
	L PrCeG	4	−49	−11	43	4.34	<0.0005
	L CeS	3	−27	−31	56	4.58	<0.0005
	L CeS	1	−53	−6	22	4.34	<0.0005
	L PoCG/PoCS	2	−14	−44	66	4.63	<0.0005
	L PCu	5/7	−8	−49	50	5.00	<0.00005
	R Cu	18	11	−85	20	6.82	<0.000001
	R SOG	18	18	−82	25	7.91	<0.000001
	R MOG	19	30	−82	6	7.13	<0.000001
	R IOG	19	43	−71	−1	7.91	<0.000001
	R CS	17	7	−86	−1	5.25	<0.00005
	R CS	17	15	−64	5	5.26	<0.00005
	R LG	18	4	−79	−2	4.92	<0.0001
	R FG	19	26	−55	−8	5.69	<0.00001
	R CeS	3	51	−12	28	4.37	<0.0005
	R PoCeG	3	9	−36	65	5.45	<0.00005
	R PoCeG	2	25	−36	56	4.78	<0.0001
	R SPL	7	21	−64	43	5.79	<0.00001
SD Task (EB > SC)	R CeS	3	19	−32	56	4.76	<0.0001

CeS, central sulcus; FG, fusiform gyrus; HG, Heschl's gyrus; MTG, middle temporal gyrus; PCu, precuneus; PrCeG, precentral gyrus; SOG, superior occipital gyrus; SPL, superior parietal lobule. All other abbreviations as in Table 2.

Figure 4. Differences between activation elicited during one-back tasks (ID + Loc) versus control task (SD) in EB and SC subjects. Differences are shown at $P < 0.05$, FDR-corrected. Color scale codes t values. In EB, auditory one-back tasks produced stronger activation in bilateral occipital cortex compared with the SD task. In SC, auditory one-back tasks produced stronger activation in nonprimary auditory cortex (left and right pSTG) than the SD task.

interactions. Significant effects of such interactions imply that activation in different ROIs (or pairs of symmetrical ROIs) may be affected by CT in one group but not another, or CT may have a different effect on activation in the EB and SC. Using the GLM revealed significant [CT × Group × ROI] and [CT × Group × ROI × Hemisphere] interactions in all 3 experimental tasks (Loc task: $F_{6,125} = 12.8$, $P < 0.0001$ and $F_{12,125} = 3.0$, $P < 0.001$; ID task: $F_{6,125} = 10.2$, $P < 0.0001$ and $F_{12,125} = 2.2$, $P < 0.05$; SD task: $F_{6,125} = 3.1$, $P < 0.01$ and $F_{12,125} = 2.3$, $P < 0.01$, respectively). In the SD, but not in the Loc or ID tasks, activation was significantly affected by the age of subjects ($F_{1,21} = 12.2$, $P < 0.01$, $F_{1,21} = 0.5$, $P = 0.50$ and $F_{1,21} = 2.1$, $P = 0.16$, respectively).

As a next step, relationships between CT and activation were further tested separately for each ROI and each group of subjects. In the group of EB, CT had a significant main effect on regional BOLD responses in the left CS ($F_{1,8} = 10.1$, $P < 0.05$) during the ID task, and in the left Cu ($F_{1,8} = 7.5$, $P < 0.05$) and left LO ($F_{1,8} = 5.4$, $P < 0.05$) during the Loc task. In the group of SC, a significant effect of CT on regional BOLD responses was detected in the left and right pSTG ($F_{1,8} = 13.6$, $P < 0.01$ and $F_{1,8} = 5.9$, $P < 0.05$, respectively) during the Loc task. In none of these regions was activation significantly affected by age,
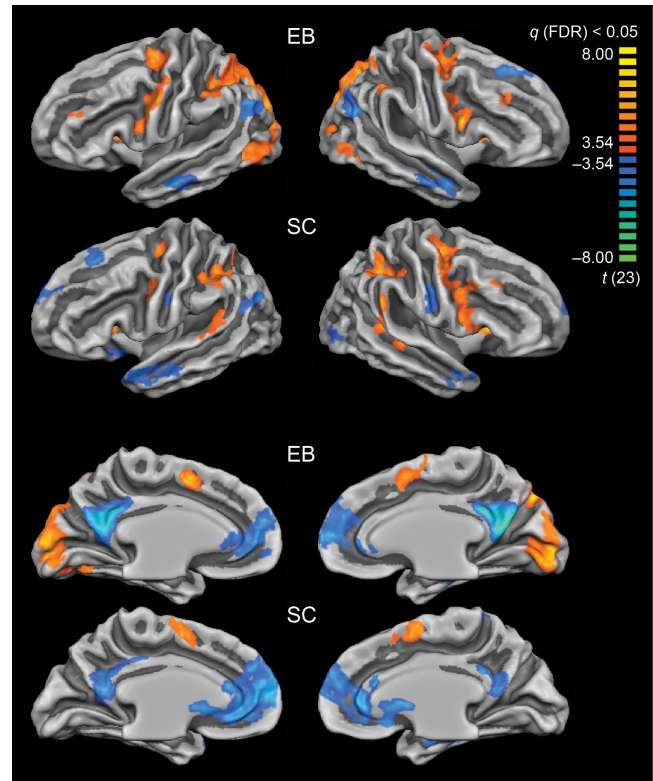
which rules out the possibility that age contributed to the relationship between CT and regional BOLD responses during the ID and Loc tasks. In contrast, activation during the SD task was significantly affected by age but not by CT in either group. In EB, age had a main effect on activation solely within left aSTG. In SC, a main effect of age was found within several occipital regions and left aSTG (Supplementary Table 1).

On the basis of the GLM results, the 5 ROIs in which CT had a significant main effect on activation during ID and Loc tasks were submitted for the next step of analysis using Pearson's correlations, in order to detect the direction of correlation between CT and activation and to calculate the correlation coefficient. In the EB group, CT correlated negatively with the magnitude of the BOLD response in several occipital regions, that is, thinner cortical regions produced stronger activation during auditory one-back tasks (Fig. 5). During the ID task, CT correlated negatively with activity in the left CS ($r = −0.67$, $P < 0.05$), whereas, during the Loc task, CT correlated negatively with activity in the left Cu ($r = −0.68$, $P < 0.05$) and left LO ($r = −0.58$, $P < 0.05$). In the group of SC, CT within the bilateral pSTG regions correlated negatively with activity during the Loc task (left and right, $r = −0.65$, $P < 0.05$).

Finally, correlations between CT and regional BOLD responses were examined at the whole-brain level (vertex by vertex). The analysis was performed for the Loc and ID tasks, in which functional activation was significantly affected by CT but not by Age, implying that Age was not a contributing factor to the relationship between CT and activation.

Table 4

Brain regions showing significant differences in activation between auditory one-back tasks (ID + Loc) and the sound-detection (SD) task in EB and SC in the whole-brain analysis

	Brain region	BA	x	y	z	t value	P value
EB							
Activations	L Cu	17	−4	−88	6	6.99	<0.000001
	L Cu	18	−12	−88	20	6.90	<0.000001
	L MOG	18	−23	−87	8	5.82	<0.00001
	L IOG	19	−39	−80	−4	5.63	<0.00001
	L CS	17	−9	−90	0	6.21	<0.000005
	L LG	18	−5	−83	−6	4.91	<0.0001
	L FG	19	−23	−65	−11	4.74	<0.0001
	L MeFG	6	−7	1	47	6.29	<0.000005
	L MFG	46	−34	42	25	4.34	<0.0005
	L PrCeG	6	−50	−2	33	6.92	<0.000001
	L PrCeS	6	−19	−11	55	5.39	<0.00005
	L aINS	13	−29	14	10	5.39	<0.00005
	L IPS	7/40	−37	−42	37	5.74	<0.00001
	R Cu	17	5	−89	8	5.54	<0.00005
	R MOG	18	30	−80	7	4.70	<0.0001
	R IOG	19	43	−71	−1	5.19	<0.00005
	R CS	17	6	−86	−1	6.12	<0.000005
	R LG	18	4	−81	−4	5.90	<0.000005
	R MFG	9/46	35	27	31	4.46	<0.0005
	R MeFG	6	9	5	50	4.86	<0.0001
	R PrCeS	6	44	4	21	6.21	<0.000005
	R PrCeG/PrCeS	4/6	38	−8	46	5.37	<0.00005
	R aINS	13	30	14	12	5.46	<0.00005
	R SPL	7	20	−75	38	6.59	<0.000001
	R SMG	40	48	−40	40	5.33	<0.00005
Deactivations	L MeFG/ACG	32	−10	47	12	−5.71	<0.00001
	L PCG	30	−8	−58	16	−6.47	<0.000001
	L AG	39	−43	−65	27	−5.15	<0.00005
	L STS/MTG	21/22	−57	−12	−12	−5.36	<0.00005
	R SFG	9	19	23	48	−4.56	<0.0005
	R MeFG/ACG	32	10	54	11	−5.20	<0.00005
	R PCG	23/30	4	−56	20	−6.82	<0.000001
	R AG	39	44	−61	24	−5.00	<0.00005
	R STS/MTG	21/22	50	−2	−18	−4.98	<0.00005
SC							
Activations	L MeFG	6	−8	0	52	5.38	<0.00005
	L PrCeG	4	−43	−4	36	4.88	<0.0001
	L PrCeS	6	−24	−15	51	4.68	<0.0005
	L aINS	13	−30	17	14	5.43	<0.00005
	L IPS	40	−49	−38	36	5.86	<0.00001
	L STG	22	−53	−40	14	4.52	<0.0005
	R MeFG	6	8	2	51	5.29	<0.00005
	R PrCeS	6	47	4	19	5.17	<0.00005
	R PrCeG/PrCeS	4/6	38	−8	47	6.29	<0.000005
	R aINS	13	29	19	12	6.21	<0.000005
	R IPS	7/40	34	−49	37	5.89	<0.000005
	R STG	42/40	56	−39	25	5.47	<0.00005
	R STS	22	44	−32	−1	4.85	<0.0001
Deactivations	L SFG	8	−16	26	47	−4.66	<0.0005
	L ACG	24/32	−6	35	6	−5.49	<0.00005
	L PCG	23/30	−5	−50	18	−4.99	<0.00005
	L CeS	3	−49	−13	29	−4.38	<0.0005
	L AG	39/19	−39	−71	23	−5.03	<0.00005
	L STG/STS	22/38	−48	6	−14	−5.19	<0.00005
	R MOG/IOG	19	39	−78	−2	−4.28	<0.0005
	R MeFG/ACG	24	5	36	8	−5.18	<0.00005
	R PCG	23	6	−42	30	−5.00	<0.00005
	R CeS	3	50	−13	31	−4.94	<0.0001
	R STG/STS	38	48	3	−15	−5.00	<0.00005

AG, angular gyrus; aINS, anterior insula; PCG, posterior cingulate gyrus; IPS, intraparietal sulcus; MeFG, medial frontal gyrus; PrCeG, precentral gyrus; PrCeS, precentral sulcus; SMG, supramarginal gyrus; STG, superior temporal gyrus; STS, superior temporal sulcus. All other abbreviations as in Tables 2–3.

In the group of EB, all significant correlations between CT and BOLD responses found during either ID or Loc tasks were negative and were observed mainly within the occipital lobes. Areas of significant correlation between CT and BOLD response during the ID task included left CS, LG, SOG, right Cu, and left middle frontal gyrus (MFG). During the Loc task, CT correlated negatively with the BOLD response in CS, LG, MOG, and SOG in the left hemisphere and Cu in the right hemisphere (Table 5, Fig. 6). In SC, negative correlations between CT and BOLD responses during the Loc task were found in the temporal and frontal lobes of the left hemisphere. Clusters of significant correlations were located in the STG, STS, temporal pole, and inferior frontal gyrus (IFG). During the ID task, CT correlated negatively with the BOLD response in left IFG and positively in right lingual/fusiform gyri on the ventral surface of the occipital lobes. Taking into account that visual cortex in SC tended to be deactivated by auditory one-back tasks, the latter positive correlation implies that thinner cortex may be suppressed more effectively.

Correlation Between Cortical Thickness and Age

In the EB group, CT correlated negatively with both age (Supplementary Fig. 2) and duration of blindness in the left HG (age: $r = −0.63$, $P < 0.05$; duration of blindness: $r = −0.63$, $P < 0.05$) and the right aSTG (age: $r = −0.77$, $P < 0.01$; duration of blindness: $r = −0.75$, $P < 0.01$). In the SC group, a significant correlation between CT and age was found only in primary visual cortex within the right CS ($r = −0.59$, $P < 0.05$).

Summary of Results

In occipital cortex, the group of EB subjects (compared with SC) showed greater CT and stronger functional activation by auditory one-back tasks (Tables 2, 3, and 6). In superior temporal cortex, these effects were mixed: left HG (which includes primary auditory cortex) was thicker in EB than SC, while nonprimary auditory cortex in left aSTG was thinner in EB than SC (Table 6). Finally, for both groups, functional activation in areas that were preferentially involved during auditory one-back tasks (occipital cortex [CS, LG, SOG, MOG, and Cu] for EB and nonprimary auditory cortex [aSTG and pSTG] for SC) correlated negatively with CT. This similarity between occipital areas in EB and nonprimary auditory areas in SC confirms our hypothesis that these areas are performing the same types of operation during demanding auditory information processing.

Discussion

We analyzed structural and functional changes in the cerebral cortex of EB subjects. To understand the relationship between structure and function, we combined measurements of CT and functional activation (regional BOLD responses). Negative correlations between CT and functional activation (i.e., stronger activation in thinner cortex) during attention-demanding auditory tasks were found in occipital cortex of EB and in nonprimary auditory cortex of sighted controls (SC). Based on classical animal studies on the effects of visual deprivation, we conclude that activity-dependent pruning and changes of synaptic efficacy are the main causes for the observed structure–function relationships in blind humans. However, other forms of plasticity, including those related to long-term practice, may contribute to these correlations as well.

Structural Correlates of Plasticity

Reduced Pruning with Early Visual Deprivation

In the group of EB, a thicker cortex (compared with SC) was found bilaterally within the LO and Cu regions of the occipital lobe, and in the left CS and LG. These results are in line with
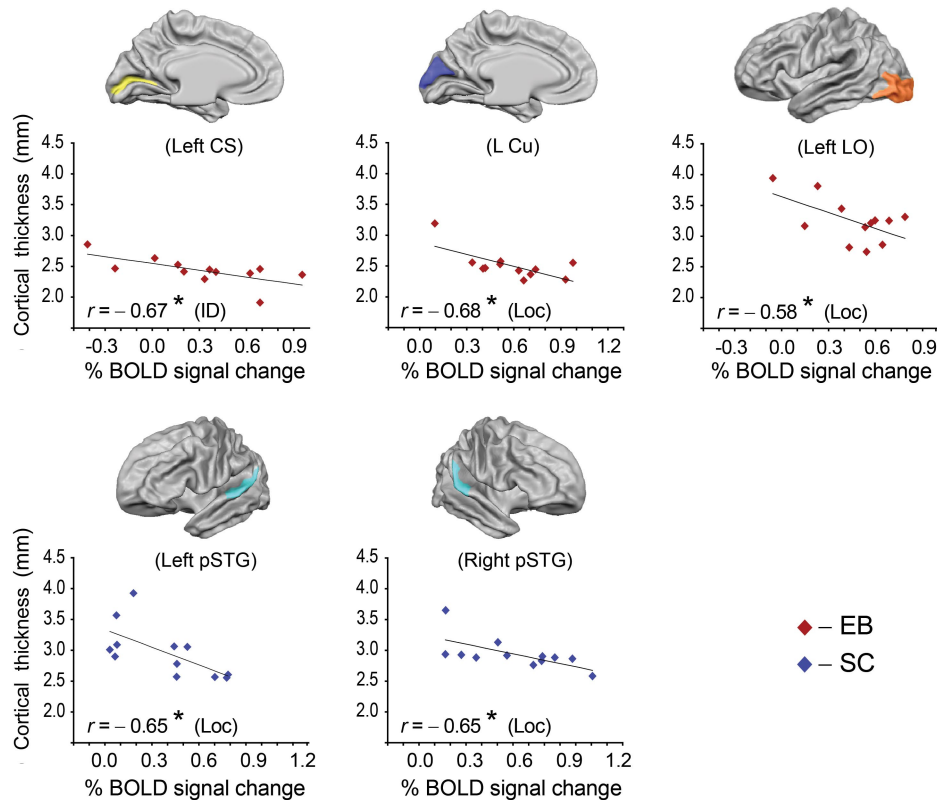
Figure 5. Correlations between cortical thickness and magnitude of BOLD response within anatomically defined ROIs, as shown above each plot. Data points for EB subjects are represented with red diamonds, for SC with blue diamonds. *r*: correlation coefficient; *P < 0.05. In all ROIs shown, CT but not Age produced a significant effect on activation.

Table 5
Brain regions showing significant correlations between CT and functional activation in EB and SC in the whole-brain analysis

Brain region	BA	x	y	z	r value	P value
EB, ID task						
L CS	17	−10	−87	0	−0.73	<0.01
L LG	18	−5	−85	−7	−0.79	<0.005
L SOG	19	−28	−81	15	−0.83	<0.001
L MFG	8	−33	19	44	−0.90	<0.0001
R Cu	18	9	−63	12	−0.79	<0.005
EB, Loc task						
L CS	17	−9	−87	−3	−0.77	<0.005
L LG	18	−5	−85	−7	−0.84	<0.001
L MOG	18	−29	−90	1	−0.79	<0.005
L SOG	19	−22	−80	21	−0.84	<0.001
R Cu	19	12	−80	35	−0.81	<0.005
SC, ID task						
R LG/FG	18	22	−86	−12	0.84	<0.001
L IFG	45	−45	34	−1	−0.85	<0.0005
SC, Loc task						
L IFG	45	−47	37	2	−0.90	<0.0001
L STG	22	−54	−6	−4	−0.86	<0.0005
L STS	21	−52	−28	−5	−0.84	<0.001
L Temp Pole	38	−46	−1	−26	−0.87	<0.0005

Temp Pole, temporal pole; IFG, inferior frontal gyrus. All other abbreviations as in Tables 2–4.

previous observations of a thicker visual cortex in early and CB individuals (Bridge et al. 2009; Jiang et al. 2009; Park et al. 2009; Voss and Zatorre 2011). Importantly, no thickening of occipital cortex was found in LB subjects, which suggests that the thickness of occipital cortex depends on early visual experience. Consistently, in PET studies, high levels of glucose metabolism related to synaptic activity were also observed in

the occipital cortex of early but not LB subjects during the resting state (Veraart et al. 1990; De Volder et al. 1997). Thus, the increased thickness in EB compared with SC may result from reduced pruning of exuberant connections during the early stages of ontogeny (Innocenti 2007; Jiang et al. 2009; Park et al. 2009; Voss and Zatorre 2011).

Results from a classical series of microscopic neuroanatomical studies in rhesus monkeys by Rakic and colleagues (Rakic et al. 1986, 1994; Bourgeois et al. 1989, 1994; Zecevic et al. 1989; Zecevic and Rakic 1991; Bourgeois and Rakic 1993, 1996), and from similar studies in humans (Huttenlocher et al. 1982; Garey 1984; Huttenlocher 1984, 1990; Huttenlocher and de Courten 1987; Huttenlocher and Dabholkar 1997) have demonstrated that the early stages of ontogeny (from the prenatal period through infancy) are characterized by an initial overproduction of synaptic contacts followed by pruning of inactive synapses. In human visual cortex, synaptogenesis is most rapid between the ages of 2–4 months and occurs concurrently with dendritic and axonal growth and with myelination of the subcortical WM (Huttenlocher and de Courten 1987; Huttenlocher and Dabholkar 1997). The initial concurrent synaptic overproduction in different cortical layers and areas (Rakic et al. 1986; Huttenlocher 1990; Huttenlocher and Dabholkar 1997) may be a prerequisite for the subsequent refinement of connections within neural circuits by mechanism of competitive interactions between extrinsic afferents (Rakic et al. 1986; Zecevic and Rakic 1991; Bourgeois et al. 1994). Maximum synaptic density in the human visual cortex is reached by age 8 months to 1 year (Garey 1984; Huttenlocher 1984).
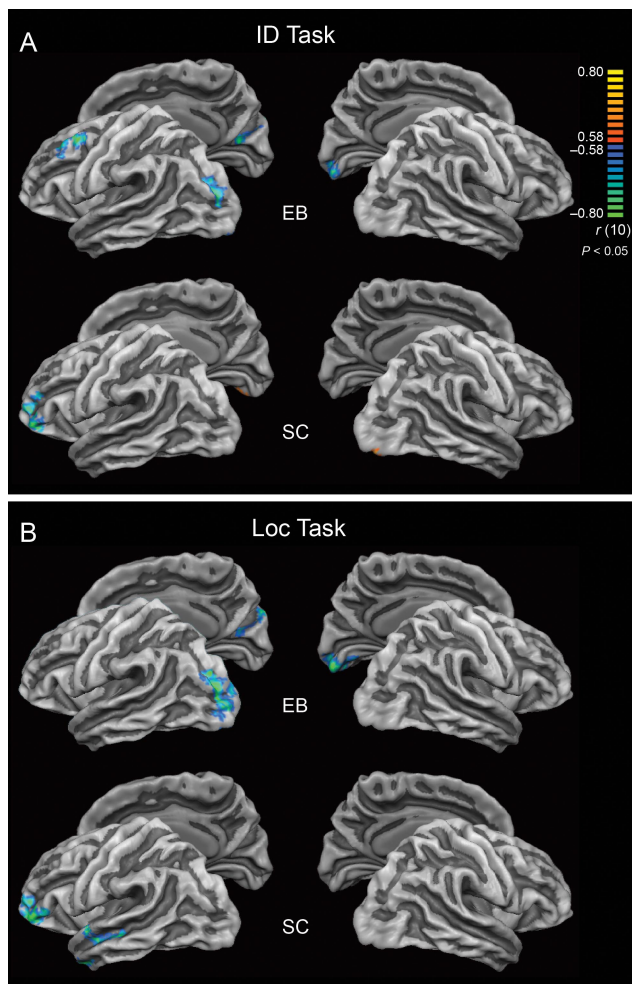
Figure 6. Whole-brain correlations between cortical thickness and magnitude of BOLD response during ID (*A*) and Loc tasks (*B*). Results are shown at $P < 0.05$, corrected by cluster size. The color scale codes *r* values. In SC, negative correlation between CT and magnitude of cortical activation during auditory one-back Loc task was observed in nonprimary auditory areas in the left temporal lobe. In EB, in contrast, clusters of significant negative correlation between CT and magnitude of cortical activation during auditory ID and Loc tasks were located in the occipital lobes.

The rapid phase of synaptogenesis is followed by a subsequent longer period of pruning, during which synapses are eliminated by about 40% to reach mature levels at about 11 years of age in humans (Huttenlocher et al. 1982; Garey 1984; Huttenlocher 1984, 1990; Huttenlocher and de Courten 1987). While the first phase of synapse formation is independent of retinal input (Bourgeois et al. 1989; Bourgeois and Rakic 1996), synaptic pruning in the retino-geniculo-striate pathway is controlled by sensory experience (Rakic et al. 1986; Stryker and Harris 1986) or, more generally, by patterned neural activity in the retinal ganglion cells (Meister et al. 1991; Wong et al. 1993). Neural activity causes not only selective survival of active synapses, but also further strengthening of synaptic efficacy, which is essential for full functional maturation of the brain (Rakic et al. 1986). Thus, the increased CT in EB compared with SC may, in large part, be due to greater survival of exuberant cortico-cortical and thalamo-cortical connections, which fail to get pruned under conditions of early sensory deprivation (Hyvärinen et al. 1981; Rauschecker and Korte 1993; Kingsbury et al. 2002; Karlen et al. 2006).

Changes of Cell Morphology with Visual Deprivation

A further source of intergroup differences in CT between EB and SC might be alteration of cellular morphology in visually deprived individuals. Results of a recent developmental study suggest that binocular enucleation in newborn ferrets causes a reduction in the proportion of stellate cells in layer IV of primary visual cortex (the main target of thalamic afferents), and a concomitant increase in the size of their basal dendrites when compared with neurons within the same layer of normally developing controls (Callaway and Borrell 2011). In sighted animals, the stellate cells of layer IV were shown to initially develop as pyramidal cells and, thereafter, transform their dendritic arborization to stellate appearance by a process of active retraction of apical dendrites paralleled by an increase in the number of basal dendrites (Vercelli et al. 1992; Callaway and Borrell 2011). In enucleated ferrets, a large proportion of neurons failed to cease growth of apical dendrites, and even neurons that eliminated their apical dendrites developed excessively large basal dendrites (Callaway and Borrell 2011). In agreement with this finding, an experiment on rabbits showed that neonatal deafening increased the nonpyramidal dendrite length in layers III/IV of primary auditory cortex by 27% relative to normally hearing controls (McMullen et al. 1988). The process of dendritic development is regulated by several neurotrophic factors, for example, brain-derived neurotrophic factor and neurotrophin 3 (McAllister et al. 1996; Callaway and Borrell 2011). The growth-promoting influence of these factors can, in turn, be affected by neuronal firing activity (McAllister et al. 1996). Consequently, congenital or early sensory deprivation may result in major remodeling of the cortical fine structure.

Structural Changes in the Auditory Cortex of the Early Blind

In auditory cortex, group differences in CT were observed in left HG, where cortex was thicker in EB than in SC, and in left aSTG, where cortex was thinner in EB. The latter finding is in line with a study by Park et al. (2009) showing a thinner nonprimary auditory cortex in CB compared with SC. Histological and neuroimaging studies suggest that the development of brain structures is heterochronous, with frontal and temporal association areas maturing last (Huttenlocher and Dabholkar 1997; Giedd et al. 1999; Gogtay et al. 2004; Sowell et al. 2004). For this reason, synaptic pruning of nonprimary auditory cortex may have a greater impact on its ultimate fine organization, resulting in greater synaptic efficacy, as reflected by higher activation levels in EB individuals compared with SC.

The Effect of Training on Cortical Thickness

In contrast to the above effects of early sensory deprivation, studies on brain plasticity in adult humans related to extensive training have reported increases in both GM volume and CT (Sluming et al. 2002; Gaser and Schlaug 2003; Draganski et al. 2004; Cannonieri et al. 2007; Bermudez et al. 2009; Jacini et al. 2009; Engvig et al. 2010; Foster and Zatorre 2010; Wei et al. 2011). This may be explained by, for example, axonal sprouting (Darian-Smith and Gilbert 1994; Gilbert and Li 2012) and increased spine density (Yuste and Bonhoeffer 2004) in structures critical for a certain skill or task performance. Left auditory cortex plays a crucial role in auditory temporal processing (Zatorre and Belin 2001; Jamison et al. 2006; Warrier et al. 2009), and the thickening of left HG observed here may be related to the acquisition of skills important for

Table 6
Summary of results

ROI		Analysis	Left hemisphere			Right hemisphere		
			CT	Activation	Correlation	CT	Activation	Correlation
Occipital cortex	CS	Whole-brain	EB > SC	EB > SC (ID, Loc) EB: ID + Loc > SD	EB: negative (ID, Loc)	n.s.	EB > SC (ID, Loc) EB: ID + Loc > SD	n.s.
		ROI	EB > SC	EB > SC (ID, Loc) EB: ID > SD, Loc > SD	EB: negative (ID)	n.s.	EB > SC (ID, Loc) EB: ID > SD, Loc > SD	n.s.
	LG	Whole-brain	EB > SC	EB > SC (ID, Loc) EB: ID + Loc > SD	EB: negative (ID, Loc)	EB > SC	EB > SC (ID, Loc) EB: ID + Loc > SD	SC: positive (ID)
		ROI	EB > SC	EB > SC (ID, Loc) EB: ID > SD, Loc > SD	n.s.	n.s.	EB > SC (ID, Loc) EB: ID > SD, Loc > SD	n.s.
	Cu	Whole-brain	EB > SC	EB > SC (ID, Loc) EB: ID + Loc > SD	n.s.	EB > SC	EB > SC (ID, Loc) EB: ID + Loc > SD	EB: negative (ID, Loc)
		ROI	EB > SC	EB > SC (ID, Loc) EB: ID > SD, Loc > SD SC: ID<SD, Loc <SD, Loc <ID	EB: negative (Loc)	EB > SC	EB > SC (ID, Loc) EB: ID > SD, Loc > SD SC: Loc <SD	n.s.
	LO	Whole-brain	EB > SC	EB > SC (ID, Loc) EB: ID + Loc > SD	EB: negative (Loc)	EB > SC	EB > SC (ID, Loc) EB: ID + Loc > SD	n.s.
		ROI	EB > SC	EB > SC (ID, Loc) EB: ID > SD, Loc > SD SC: ID<SD, Loc <SD	EB: negative (Loc)	EB > SC	EB > SC (ID, Loc) EB: ID > SD, Loc > SD SC: ID<SD, Loc <SD	n.s.
Superior temporal cortex	HG	Whole-brain	n.s.	EB < SC (ID)	n.s.	n.s.	n.s.	n.s.
		ROI	EB > SC	EB < SC (ID)	n.s.	n.s.	n.s.	n.s.
	STGa	Whole-brain	n.s.	n.s.	SC: negative (Loc)	n.s.	n.s.	n.s.
		ROI	EB < SC	EB > SC	n.s.	n.s.	SC: ID > Loc	n.s.
	STGp	Whole-brain	n.s.	SC: ID + Loc > SD	n.s.	n.s.	SC: ID + Loc > SD	n.s.
		ROI	n.s.	SC: ID > SD, Loc > SD	SC: negative (Loc)	n.s.	SC: ID > SD, Loc > SD	SC: negative (Loc)

n.s., no significant difference; ROI, region of interest.

social communication in EB, for instance, comprehension of ultra-fast speech exploited in assistive devices (Moos et al. 2008; Hertrich et al. 2009).

Functional Correlates of Plasticity

In line with several neuroimaging and electrophysiological studies (Kujala et al. 1995, 2005; Sadato et al. 1996, 1998; Weeks et al. 2000; Amedi et al. 2003; Bedny et al. 2011), functional reorganization of occipital areas in EB was reflected in the consistent involvement of these areas during tasks requiring auditory selective attention and working memory, whereas simple sound detection elicited less reliable activation within occipital cortex. These findings are also in line with a recent study on congenitally deaf subjects, which demonstrated that more demanding, bimodal tasks elicited stronger activation of the deprived auditory cortex than less demanding unimodal tasks (Karns et al. 2012).

While activity within nonprimary auditory areas of SC was modulated by the type of task and varied across experimental conditions, blind subjects showed less differentiation. Higher level functions of auditory cognition, normally accomplished by nonprimary auditory areas (Rauschecker and Scott 2009), may be taken on by occipital regions in EB. Results from several recent studies in CB and EB subjects demonstrate that occipital areas in the deprived dorsal "visual" where-pathway remain specialized for the processing of spatial characteristics (Renier et al. 2010; Collignon et al. 2011) and motion in space (Poirier et al. 2006; Bedny et al. 2010; Wolbers et al. 2011), while switching their modality to the auditory domain. In the context of the present study, this suggests that large regions of occipital cortex may in fact be innately multisensory and, in EB, take over functions of nonprimary auditory areas in auditory cognitive tasks. These functions are specified, however, by the computational algorithms that each area has built in regardless of sensory modality.

The above cross-modal organizational principles may be generalized to other sensory modalities (Renier et al. 2013). This is strongly supported by recent animal studies on congenital and early deafness (Lomber et al. 2010, 2011; Meredith et al. 2011). The authors demonstrated superior visual spatial abilities in early deaf cats. Reversible cooling of the posterior auditory field, which is normally involved in sound localization in hearing animals (Lomber and Malhotra 2008), selectively eliminated the superior visual localization abilities of the deaf animals, whereas deactivation of the dorsal zone of "auditory" cortex disrupted their superior visual motion detection abilities. Thus, in very general terms, the original functions of nonprimary sensory areas seem to be preserved after sensory deprivation, although the modalities driving the neurons in the reorganized areas are altered (Lomber et al. 2010, 2011; Renier et al. 2010, 2013; Kok et al. 2014).

Correlation Between Structure and Age

We found negative correlations between CT and age in both groups: In SC within primary visual cortex and in EB in both primary and nonprimary auditory cortex. CT in the CS of primary visual cortex has been shown to decrease during the lifespan; moreover, CS is among the cortical areas that are thinning most rapidly with age (Salat et al. 2004). In EB, however, no significant correlations between CT and either age or duration of blindness were found in any of the occipital ROIs.

In a recent study by Voss and Zatorre (2011), CT in the occipital lobe was shown to correlate positively with the duration of blindness in a joint group of EB and LB subjects, implying that exuberant connections might be utilized and strengthened to compensate for the vision loss through experience-dependent plasticity. A stable CT of the occipital lobes in our quite homogenous group of EB subjects may reflect the superposition of two opposing trends: a decrease of CT due to developmental maturation and aging, and an

increase due to experience-dependent plasticity and training, which results in thickening of cortex and thus compensates for age-related thinning.

On the other hand, the thickness of auditory cortex in EB did correlate negatively with age. This suggests that cortical areas corresponding to the ecologically most important input channel in the blind, carrying, for example, distance information, may be affected more strongly by individual experience.

Correlation Between Structure and Function

The main finding of the present study is a consistent negative correlation between the magnitude of activation and CT in EB subjects, that is, stronger activations are generally found in thinner cortex. This is in line with recent developmental studies (Lu et al. 2009; Nunez et al. 2011) demonstrating a similar relationship in fronto-parietal areas of children of various ages performing linguistic tasks. Both sets of results suggest that pruning of exuberant connections during development increases selectivity and effectiveness of synaptic activity and, therefore, leads to stronger activation.

From this perspective, it is noteworthy that negative correlations between CT and functional activation were observed for both EB as for SC during the Loc (but not the ID) task in areas known to be involved in auditory spatial processing: pSTG in the sighted (as revealed by ROI analysis) and MOG in the blind volunteers (as revealed by both ROI and whole-brain analyses). This finding suggests that the aforementioned areas are adapted for optimal processing of auditory spatial features and further supports a specific role of the MOG in auditory localization following congenital or early blindness.

Individual experience may also affect structure–function relationship, but these effects are not uniform. Long-term practice may increase CT and reduce activation (Meister et al. 2005; Haier et al. 2009) leading again to negative correlations between the two measures. However, long-term training may also result in increases of activation (Koelsch et al. 2005), as demonstrated for musicians in areas that were thicker in musicians than nonmusicians (Bermudez et al. 2009). Thus, intense training may sometimes result in the opposite structure–function relationships, masking the effects of pruning to a certain extent.

Effects of Age

What complicates matters further is that experience-dependent changes are superimposed on regular aging-related changes, such as cellular shrinkage and reduction in dendritic arborization (Morrison and Hof 1997). Thus, age per se also contributes to negative correlations between CT and activation. Sensory cortical areas have been shown to undergo relatively linear thinning throughout the lifespan (Salat et al. 2004; Sowell et al. 2007). At the same time, functional neuroimaging studies have consistently shown that senior subjects produce overactivations in a wide range of perceptual, motoric, mnemonic, and verbal tasks, apparently in an effort to compensate for age-related decline (Cabeza 2001; Reuter-Lorenz and Cappell 2008). Although overactivations in the older group were predominantly confined to the fronto-parietal network, some authors also reported additional overactivations in non-primary visual and auditory areas (Grady et al. 1994; Townsend et al. 2006).

In the present study, analysis of the relationship between CT and functional activation was controlled for age by using age as a continuous predictor in a mixed-effects GLM. Since age did not affect magnitude of BOLD responses during either ID or Loc tasks, the possibility that it contributed significantly to the relationship between CT and activation during working memory processing of auditory attributes can be discounted.

Conclusions

The present study provides evidence for both structural and functional reorganization of the visual and auditory cortex in EB individuals. In addition, our results demonstrate negative correlations between CT and BOLD response magnitude in areas involved in demanding processing of auditory information: occipital cortex in EB and pSTG in SC. The findings of the present study imply an important role of occipital cortex as a substrate for higher order processing of auditory information in visually deprived individuals. In addition, both primary and nonprimary auditory areas, with their potential for multisensory integration (Hackett and Schroeder 2009), provide an extended capacity in EB for detailed sensory processing of sounds. Together, these mechanisms may underlie the superior performance of blind individuals in perceptually difficult tasks.

Supplementary Material

Funding

Notes

Conflict of Interest: None declared.

References

Amedi A, Raz N, Pianka P, Malach R, Zohary E. 2003. Early "visual" cortex activation correlates with superior verbal memory performance in the blind. Nat Neurosci. 6:758–766.

Bavelier D, Neville HJ. 2002. Cross-modal plasticity: where and how? Nat Rev Neurosci. 3:443–452.

Bedny M, Konkle T, Pelphrey K, Saxe R, Pascual-Leone A. 2010. Sensitive period for a multimodal response in human visual motion area MT/MST. Curr Biol. 20:1900–1906.

Bedny M, Pascual-Leone A, Dodell-Feder D, Fedorenko E, Saxe R. 2011. Language processing in the occipital cortex of congenitally blind adults. Proc Natl Acad Sci USA. 108:4429–4434.

Bermudez P, Lerch JP, Evans AC, Zatorre RJ. 2009. Neuroanatomical correlates of musicianship as revealed by cortical thickness and voxel-based morphometry. Cereb Cortex. 19:1583–1596.

Bridge H, Cowey A, Ragge N, Watkins K. 2009. Imaging studies in congenital anophthalmia reveal preservation of brain architecture in 'visual' cortex. Brain. 132:3467–3480.

Büchel C, Price C, Friston K. 1998. A multimodal language region in the ventral visual pathway. Nature. 394:274–277.

Buckner RL, Andrews-Hanna JR, Schacter DL. 2008. The brain's default network: anatomy, function, and relevance to disease. Ann N Y Acad Sci. 1124:1–38.

Burton H, Diamond JB, McDermott KB. 2003. Dissociating cortical regions activated by semantic and phonological tasks: a fMRI study in blind and sighted people. J Neurophysiol. 90:1965–1982.

Bourgeois JP, Goldman-Rakic PS, Rakic P. 1994. Synaptogenesis in the prefrontal cortex of rhesus monkeys. Cereb Cortex. 4:78–96.

Bourgeois JP, Jastreboff PJ, Rakic P. 1989. Synaptogenesis in visual cortex of normal and preterm monkeys: evidence for intrinsic regulation of synaptic overproduction. Proc Natl Acad Sci USA. 86:4297–4301.

Bourgeois JP, Rakic P. 1993. Changes of synaptic density in the primary visual cortex of the macaque monkey from fetal to adult stage. J Neurosci. 13:2801–2820.

Bourgeois JP, Rakic P. 1996. Synaptogenesis in the occipital cortex of macaque monkey devoid of retinal input from early embryonic stages. Eur J Neurosci. 8:942–950.

Cabeza R. 2001. Cognitive neuroscience of aging: contributions of functional neuroimaging. Scand J Psychol. 42:277–286.

Callaway EM, Borrell V. 2011. Developmental sculpting of dendritic morphology of layer 4 neurons in visual cortex: influence of retinal input. J Neurosci. 31:7456–7470.

Cannonieri GC, Bonilha L, Fernandes PT, Cendes F, Li LM. 2007. Practice and perfect: length of training and structural brain changes in experienced typists. Neuroreport. 18:1063–1066.

Cohen LG, Celnik P, Pascual-Leone A, Corwell B, Falz L, Dambrosia J, Honda M, Sadato N, Gerloff C, Catala MD et al. 1997. Functional relevance of cross-modal plasticity in blind humans. Nature. 389:180–183.

Collignon O, Vandewalle G, Voss P, Albouy G, Charbonneau G, Lassonde M, Lepore F. 2011. Functional specialization for auditory-spatial processing in the occipital cortex of congenitally blind humans. Proc Natl Acad Sci USA. 108:4435–4440.

Darian-Smith C, Gilbert CD. 1994. Axonal sprouting accompanies functional reorganization in adult cat striate cortex. Nature. 368:737–740.

De Volder AG, Bol A, Blin J, Robert A, Arno P, Grandin C, Michel C, Veraart C. 1997. Brain energy metabolism in early blind subjects: neural activity in the visual cortex. Brain Res. 750:235–244.

Draganski B, Gaser C, Busch V, Schuierer G, Bogdahn U, May A. 2004. Neuroplasticity: changes in grey matter induced by training. Nature. 427:311–312.

Engvig A, Fjell AM, Westlye LT, Moberget T, Sundseth O, Larsen VA, Walhovd KB. 2010. Effects of memory training on cortical thickness in the elderly. Neuroimage. 52:1667–1676.

Foster NE, Zatorre RJ. 2010. Cortical structure predicts success in performing musical transformation judgments. Neuroimage. 53:26–36.

Garey LJ. 1984. Structural development of the visual system of man. Hum Neurobiol. 3:75–80.

Gaser C, Schlaug G. 2003. Brain structures differ between musicians and non-musicians. J Neurosci. 23:9240–9245.

Geuze E, Westenberg HG, Heinecke A, de Kloet CS, Goebel R, Vermetten E. 2008. Thinner prefrontal cortex in veterans with posttraumatic stress disorder. Neuroimage. 41:675–681.

Giedd JN, Blumenthal J, Jeffries NO, Castellanos FX, Liu H, Zijdenbos A, Paus T, Evans AC, Rapoport JL. 1999. Brain development during childhood and adolescence: a longitudinal MRI study. Nat Neurosci. 2:861–863.

Gilbert CD, Li W. 2012. Adult visual cortical plasticity. Neuron. 75:250–264.

Gilbert CD, Wiesel TN. 1992. Receptive field dynamics in adult primary visual cortex. Nature. 356:150–152.

Goebel R, Esposito F, Formisano E. 2006. Analysis of functional image analysis contest (FIAC) data with brainvoyager QX: from single-subject to cortically aligned group general linear model analysis and self-organizing group independent component analysis. Hum Brain Mapp. 27:392–401.

Gogtay N, Giedd JN, Lusk L, Hayashi KM, Greenstein D, Vaituzis AC, Nugent TF 3rd, Herman DH, Clasen LS, Toga AW et al. 2004. Dynamic mapping of human cortical development during childhood through early adulthood. Proc Natl Acad Sci USA. 101:8174–8179.

Gougoux F, Zatorre RJ, Lassonde M, Voss P, Lepore F. 2005. A functional neuroimaging study of sound localization: visual cortex activity predicts performance in early-blind individuals. PLoS Biol. 3:e27.

Grady CL, Maisog JM, Horwitz B, Ungerleider LG, Mentis MJ, Salerno JA, Pietrini P, Wagner E, Haxby JV. 1994. Age-related changes in cortical blood flow activation during visual processing of faces and location. J Neurosci. 14:1450–1462.

Hackett TA, Schroeder CE. 2009. Multisensory integration in auditory and auditory-related areas of cortex. Hear Res. 258:1–3.

Haier RJ, Karama S, Leyba L, Jung RE. 2009. MRI assessment of cortical thickness and functional activity changes in adolescent girls following three months of practice on a visual-spatial task. BMC Res Notes. 2:174.

Hamilton RH, Pascual-Leone A. 1998. Cortical plasticity associated with Braille learning. Trends Cogn Sci. 2:168–174.

Hegarty CE, Foland-Ross LC, Narr KL, Townsend JD, Bookheimer SY, Thompson PM, Altshuler LL. 2012. Anterior cingulate activation relates to local cortical thickness. Neuroreport. 23:420–424.

Hertrich I, Dietrich S, Moos A, Trouvain J, Ackermann H. 2009. Enhanced speech perception capabilities in a blind listener are associated with activation of fusiform gyrus and primary visual cortex. Neurocase. 15:163–170.

Huttenlocher PR. 1990. Morphometric study of human cerebral cortex development. Neuropsychologia. 28:517–527.

Huttenlocher PR. 1984. Synapse elimination and plasticity in developing human cerebral cortex. Am J Ment Defic. 88:488–496.

Huttenlocher PR, Dabholkar AS. 1997. Regional differences in synaptogenesis in human cerebral cortex. J Comp Neurol. 387:167–178.

Huttenlocher PR, de Courten C. 1987. The development of synapses in striate cortex of man. Hum Neurobiol. 6:1–9.

Huttenlocher PR, de Courten C, Garey LJ, Van der Loos H. 1982. Synaptogenesis in human visual cortex—evidence for synapse elimination during normal development. Neurosci Lett. 33:247–252.

Hyvärinen J, Carlson S, Hyvärinen L. 1981. Early visual deprivation alters modality of neuronal responses in area 19 of monkey cortex. Neurosci Lett. 26:239–243.

Innocenti GM. 2007. Subcortical regulation of cortical development: some effects of early, selective deprivations. Prog Brain Res. 164:23–37.

Innocenti GM, Frost DO. 1979. Effects of visual experience on the maturation of the efferent system to the corpus callosum. Nature. 280:231–234.

Innocenti GM, Price DJ. 2005. Exuberance in the development of cortical networks. Nat Rev Neurosci. 6:955–965.

Jacini WF, Cannonieri GC, Fernandes PT, Bonilha L, Cendes F, Li LM. 2009. Can exercise shape your brain? Cortical differences associated with judo practice. J Sci Med Sport. 12:688–690.

Jamison HL, Watkins KE, Bishop DV, Matthews PM. 2006. Hemispheric specialization for processing auditory nonspeech stimuli. Cereb Cortex. 16:1266–1275.

Jiang J, Zhu W, Shi F, Liu Y, Li J, Qin W, Li K, Yu C, Jiang T. 2009. Thick visual cortex in the early blind. J Neurosci. 29:2205–2211.

Jones SE, Buchbinder BR, Aharon I. 2000. Three-dimensional mapping of cortical thickness using Laplace's equation. Hum Brain Mapp. 11:12–32.

Karlen SJ, Kahn DM, Krubitzer L. 2006. Early blindness results in abnormal corticocortical and thalamocortical connections. Neuroscience. 142:843–858.

Karni A, Meyer G, Jezzard P, Adams MM, Turner R, Ungerleider LG. 1995. Functional MRI evidence for adult motor cortex plasticity during motor skill learning. Nature. 377:155–158.

Karns CM, Dow MW, Neville HJ. 2012. Altered cross-modal processing in the primary auditory cortex of congenitally deaf adults: a visual-somatosensory fMRI study with a double-flash illusion. J Neurosci. 32:9626–9638.

Kingsbury MA, Lettman NA, Finlay BL. 2002. Reduction of early thalamic input alters adult corticocortical connectivity. Brain Res Dev Brain Res. 138:35–43.

Koelsch S, Fritz T, Schulze K, Alsop D, Schlaug G. 2005. Adults and children processing music: an fMRI study. Neuroimage. 25:1068–1076.

Kok MA, Chabot N, Lomber SG. 2014. Crossmodal reorganization of cortical afferents to dorsal auditory cortex following early- and late-onset deafness. J Comp Neurol. 522:654–675.

Kujala T, Huotilainen M, Sinkkonen J, Ahonen AI, Alho K, Hämäläinen MS, Ilmoniemi RJ, Kajola M, Knuutila JE, Lavikainen J. et al. 1995. Visual cortex activation in blind humans during sound discrimination. Neurosci Lett. 183:143–146.

Kujala T, Palva MJ, Salonen O, Alku P, Huotilainen M, Jarvinen A, Näätänen R. 2005. The role of blind humans' visual cortex in auditory change detection. Neurosci Lett. 379:127–131.

Lomber SG, Malhotra S. 2008. Double dissociation of 'what' and 'where' processing in auditory cortex. Nat Neurosci. 11:609–616.

Lomber SG, Meredith MA, Kral A. 2011. Adaptive crossmodal plasticity in deaf auditory cortex: areal and laminar contributions to supranormal vision in the deaf. Prog Brain Res. 191:251–270.

Lomber SG, Meredith MA, Kral A. 2010. Cross-modal plasticity in specific auditory cortices underlies visual compensations in the deaf. Nat Neurosci. 13:1421–1427.

Lu LH, Dapretto M, O'Hare ED, Kan E, McCourt ST, Thompson PM, Toga AW, Bookheimer SY, Sowell ER. 2009. Relationships between brain activation and brain structure in normally developing children. Cereb Cortex. 19:2595–2604.

McAllister AK, Katz LC, Lo DC. 1996. Neurotrophin regulation of cortical dendritic growth requires activity. Neuron. 17:1057–1064.

McMullen NT, Goldberger B, Suter CM, Glaser EM. 1988. Neonatal deafening alters nonpyramidal dendrite orientation in auditory cortex: a computer microscope study in the rabbit. J Comp Neurol. 267:92–106.

Meister I, Krings T, Foltys H, Boroojerdi B, Muller M, Topper R, Thron A. 2005. Effects of long-term practice and task complexity in musicians and nonmusicians performing simple and complex motor tasks: implications for cortical motor organization. Hum Brain Mapp. 25:345–352.

Meister M, Wong RO, Baylor DA, Shatz CJ. 1991. Synchronous bursts of action potentials in ganglion cells of the developing mammalian retina. Science. 252:939–943.

Merabet LB, Pascual-Leone A. 2010. Neural reorganization following sensory loss: the opportunity of change. Nat Rev Neurosci. 11:44–52.

Meredith MA, Kryklywy J, McMillan AJ, Malhotra S, Lum-Tai R, Lomber SG. 2011. Crossmodal reorganization in the early deaf switches sensory, but not behavioral roles of auditory cortex. Proc Natl Acad Sci USA. 108:8856–8861.

Moos A, Hertrich I, Dietrich S, Trouvain J, Ackermann H. 2008. Perception of ultra-fast speech by a blind listener—does he use his visual system? 8th International Speech Production Seminar (ISSP 2008), 8–12 December, Strasbourg, France, pp. 297–300.

Morrison JH, Hof PR. 1997. Life and death of neurons in the aging brain. Science. 278:412–419.

Nunez SC, Dapretto M, Katzir T, Starr A, Bramen J, Kan E, Bookheimer S, Sowell ER. 2011. fMRI of syntactic processing in typically developing children: structural correlates in the inferior frontal gyrus. Dev Cogn Neurosci. 1:313–323.

Park HJ, Lee JD, Kim EY, Park B, Oh MK, Lee S, Kim JJ. 2009. Morphological alterations in the congenital blind based on the analysis of cortical thickness and surface area. Neuroimage. 47:98–106.

Pietrini P, Furey ML, Ricciardi E, Gobbini MI, Wu WH, Cohen L, Guazzelli M, Haxby JV. 2004. Beyond sensory images: object-based representation in the human ventral pathway. Proc Natl Acad Sci USA. 101:5658–5663.

Poirier C, Collignon O, Scheiber C, Renier L, Vanlierde A, Tranduy D, Veraart C, De Volder AG. 2006. Auditory motion perception activates visual motion areas in early blind subjects. Neuroimage. 31:279–285.

Rakic P, Bourgeois JP, Eckenhoff MF, Zecevic N, Goldman-Rakic PS. 1986. Concurrent overproduction of synapses in diverse regions of the primate cerebral cortex. Science. 232:232–235.

Rakic P, Bourgeois JP, Goldman-Rakic PS. 1994. Synaptic development of the cerebral cortex: implications for learning, memory, and mental illness. Prog Brain Res. 102:227–243.

Rasser PE, Johnston P, Lagopoulos J, Ward PB, Schall U, Thienel R, Bender S, Toga AW, Thompson PM. 2005. Functional MRI BOLD response to Tower of London performance of first-episode schizophrenia patients using cortical pattern matching. Neuroimage. 26:941–951.

Rauschecker JP. 1995. Compensatory plasticity and sensory substitution in the cerebral cortex. Trends Neurosci. 18:36–43.

Rauschecker JP. 1991. Mechanisms of visual plasticity: Hebb synapses, NMDA receptors, and beyond. Physiol Rev. 71:587–615.

Rauschecker JP, Korte M. 1993. Auditory compensation for early blindness in cat cerebral cortex. J Neurosci. 13:4538–4548.

Rauschecker JP, Scott SK. 2009. Maps and streams in the auditory cortex: nonhuman primates illuminate human speech processing. Nat Neurosci. 12:718–724.

Renier LA, Anurova I, De Volder AG, Carlson S, VanMeter J, Rauschecker JP. 2010. Preserved functional specialization for spatial processing in the middle occipital gyrus of the early blind. Neuron. 68:138–148.

Renier L, De Volder AG, Rauschecker JP. 2013. Cortical plasticity and preserved function in early blindness. Neurosci Biobehav Rev. doi: 10.1016/j.neubiorev.2013.01.025.

Reuter-Lorenz PA, Cappell KA. 2008. Neurocognitive aging and the compensation hypothesis. Curr Dir Psychol Sci. 17:177–182.

Röder B, Stock O, Bien S, Neville H, Rosler F. 2002. Speech processing activates visual cortex in congenitally blind humans. Eur J Neurosci. 16:930–936.

Sadato N, Pascual-Leone A, Grafman J, Deiber MP, Ibanez V, Hallett M. 1998. Neural networks for Braille reading by the blind. Brain. 121:1213–1229.

Sadato N, Pascual-Leone A, Grafman J, Ibanez V, Deiber MP, Dold G, Hallett M. 1996. Activation of the primary visual cortex by Braille reading in blind subjects. Nature. 380:526–528.

Salat DH, Buckner RL, Snyder AZ, Greve DN, Desikan RS, Busa E, Morris JC, Dale AM, Fischl B. 2004. Thinning of the cerebral cortex in aging. Cereb Cortex. 14:721–730.

Sanes DH, Reh TA, Harris WA. 2006. The development of the nervous system. 2nd ed. Burlington (MA): Elsevier Academic Press.

Sluming V, Barrick T, Howard M, Cezayirli E, Mayes A, Roberts N. 2002. Voxel-based morphometry reveals increased gray matter density in Broca's area in male symphony orchestra musicians. Neuroimage. 17:1613–1622.

Sowell ER, Peterson BS, Kan E, Woods RP, Yoshii J, Bansal R, Xu D, Zhu H, Thompson PM, Toga AW. 2007. Sex differences in cortical thickness mapped in 176 healthy individuals between 7 and 87 years of age. Cereb Cortex. 17:1550–1560.

Sowell ER, Thompson PM, Leonard CM, Welcome SE, Kan E, Toga AW. 2004. Longitudinal mapping of cortical thickness and brain growth in normal children. J Neurosci. 24:8223–8231.

Striem-Amit E, Cohen L, Dehaene S, Amedi A. 2012. Reading with sounds: sensory substitution selectively activates the visual word form area in the blind. Neuron. 76:640–652.

Stryker MP, Harris WA. 1986. Binocular impulse blockade prevents the formation of ocular dominance columns in cat visual cortex. J Neurosci. 6:2117–2133.

Talairach G, Tournoux P. 1988. Co-planar stereotaxic atlas of the human brain. Stuttgart (NY): Georg Thieme /Thieme Medical Publishers.

Townsend J, Adamo M, Haist F. 2006. Changing channels: an fMRI study of aging and cross-modal attention shifts. Neuroimage. 31:1682–1692.

Veraart C, De Volder AG, Wanet-Defalque MC, Bol A, Michel C, Goffinet AM. 1990. Glucose utilization in human visual cortex is respectively elevated and decreased in early versus late blindness. Brain Res. 510:115–121.

Vercelli A, Assal F, Innocenti GM. 1992. Emergence of callosally projecting neurons with stellate morphology in the visual cortex of the kitten. Exp Brain Res. 90:346–358.

Voss P, Gougoux F, Zatorre RJ, Lassonde M, Lepore F. 2008. Differential occipital responses in early- and late-blind individuals during a sound-source discrimination task. Neuroimage. 40:746–758.

Voss P, Zatorre RJ. 2011. Occipital cortical thickness predicts performance on pitch and musical tasks in blind individuals. Cereb Cortex. 22:2455–2465.

Warrier C, Wong P, Penhune V, Zatorre R, Parrish T, Abrams D, Kraus N. 2009. Relating structure to function: Heschl's gyrus and acoustic processing. J Neurosci. 29:61–69.

Weeks R, Horwitz B, Aziz-Sultan A, Tian B, Wessinger CM, Cohen LG, Hallett M, Rauschecker JP. 2000. A positron emission tomographic study of auditory localization in the congenitally blind. J Neurosci. 20:2664–2672.

Wei G, Zhang Y, Jiang T, Luo J. 2011. Increased cortical thickness in sports experts: a comparison of diving players with the controls. PLoS One. 6:e17112.

Wolbers T, Zahorik P, Giudice NA. 2011. Decoding the direction of auditory motion in blind humans. Neuroimage. 56:681–687.

Wong RO, Meister M, Shatz CJ. 1993. Transient period of correlated bursting activity during development of the mammalian retina. Neuron. 11:923–938.

Yuste R, Bonhoeffer T. 2004. Genesis of dendritic spines: insights from ultrastructural and imaging studies. Nat Rev Neurosci. 5:24–34.

Zatorre RJ, Belin P. 2001. Spectral and temporal processing in human auditory cortex. Cereb Cortex. 11:946–953.

Zecevic N, Bourgeois JP, Rakic P. 1989. Changes in synaptic density in motor cortex of rhesus monkey during fetal and postnatal life. Brain Res Dev Brain Res. 50:11–32.

Zecevic N, Rakic P. 1991. Synaptogenesis in monkey somatosensory cortex. Cereb Cortex. 1:510–523.